

The prospects for magnetohydrodynamic stability in advanced tokamak regimes*

J. Manickam,[†] M. S. Chance, S. C. Jardin, C. Kessel, D. Monticello, N. Pomphrey, A. Reiman, C. Wang,^{a)} and L. E. Zakharov
Princeton Plasma Physics Laboratory, Princeton, New Jersey 08543

(Received 9 November 1993; accepted 19 January 1994)

Stability analysis of advanced regime tokamaks is presented. Here advanced regimes are defined to include configurations where the ratio of the bootstrap current, I_{BS} , to the total plasma current, I_p , approaches unity, and the normalized stored energy, $\beta_N^* = 80\pi\langle p^2 \rangle^{1/2}a/I_p B_0$, has a value greater than 4.5. Here, p is the plasma pressure, a the minor radius in meters, I_p is in mega-amperes, B_0 is the magnetic field in Tesla, and $\langle \cdot \rangle$ represents a volume average. Specific scenarios are discussed in the context of Toroidal Physics Experiment (TPX) [*Proceedings of the 20th European Physical Society Conference on Controlled Fusion and Plasma Physics*, Lisbon, 1993, edited by J. A. Costa Cabral, M. E. Manso, F. M. Serra, and F. C. Schuller (European Physical Society, Petit-Lancy, 1993), p. I-80]. The best scenario is one with reversed shear, in the q profile, in the central region of the tokamak. The bootstrap current obtained from the plasma profiles provides 90% of the required current, and is well aligned with the optimal current profile for ideal magnetohydrodynamic stability. This configuration is stable up to $\beta_N^* \approx 6.8$, if the external boundary conditions are relaxed to those corresponding to an ideal structure at a moderate distance of approximately 1.3 times the minor radius.

I. INTRODUCTION

The economic competitiveness of tokamak reactors can be enhanced by achieving the highest possible stable value of β^* while simultaneously minimizing the external sources of current drive. Here $\beta^* = 2\mu_0\langle p^2 \rangle^{1/2}/B_0^2$ is a measure of the fusion reactivity of the plasma, with p representing the plasma pressure, B_0 the vacuum magnetic field at the geometric center of the plasma, and $\langle \cdot \rangle$ represents a volume average. Another useful measure of the stored energy in a plasma is, $\beta \equiv 2\mu_0\langle p \rangle/B_0^2$. It is related to β^* through a parameter describing the peakedness of the pressure profile, $p(0)/\langle p \rangle$, where $p(0)$ is the pressure at the magnetic axis, we will use both definitions as appropriate in this report. For the equilibria discussed in this report an approximate empirical relation between them is given by the expression, $\beta^* = \beta[0.8 + 0.17p(0)/\langle p \rangle]$. In the context of magnetohydrodynamic (MHD) stability the ratio of β to the quantity I_p/aB_0 , often referred to as the Troyon coefficient, β_N , is a useful measure. It can also be expressed as $\beta_N \equiv 80\pi\langle p \rangle a/I_p B_0$, where a is the minor radius measured in meters, I_p is measured in mega-amperes, B_0 in Tesla. We will refer to the property, $\beta_N > 3.5$, as a feature of the advanced tokamak regime. This corresponds approximately to $\beta^* > 4.5I_p/(aB_0)$.

The current drive requirement can be reduced to acceptable levels, for steady-state operation, by fully utilizing the bootstrap driven current, I_{BS} . It is clearly desirable to obtain, $f_{BS} \equiv I_{BS}/I_p \approx 1$. In the past, several studies have sought to maximize the β limit from the MHD stability

viewpoint, and considerable literature describing the desirable profile features for β optimization is available.¹⁻³ However these studies paid scant attention to related bootstrap current issues. The two principal issues are, the value of f_{BS} and the detailed profile distribution. In particular it should be noted that while it is relatively easy to design a plasma configuration with $f_{BS} \sim 1$, aligning the bootstrap current with an MHD stable profile is much more difficult. With this in mind, we define the regime where these criteria, i.e., high β^* , and high f_{BS} with good alignment, are satisfied to be the advanced tokamak regime. Accessing this regime is one of the missions of Toroidal Physics Experiment (TPX).⁴ It is a diverted tokamak which has an aspect ratio of 4.5, with a major radius, $R=2.25$ m, and a minor radius, $a=0.5$ m. The cross section is D shaped with an elongation of 1.8 and triangularity equal to 0.5, when measured at the flux surface which corresponds to 95% of the flux difference between the magnetic axis and the separatrix. The magnetic field is designed to be 4 T at $R=2.25$ m, and it is capable of carrying a plasma current up to 2 MA. We present the results of extensive theoretical searches for plasma configurations in the advanced tokamak regime, in the context of TPX.

The β limit is set by one of several ideal MHD instabilities.

In order to determine the β limit it is necessary to determine the stability of the equilibrium with respect to several ideal MHD instabilities. These include, modes with toroidal mode number ranging from 1 to ∞ , under the influence of a variety of appropriate boundary conditions. The equilibrium with the lowest threshold sets the β limit, which will be designated here as β_{N1}^* with a corresponding value of β_{N1}^* . In practice it is sufficient to analyze modes with $1 \leq n \leq 5$ and at the high- n limit, the ballooning modes. Note that the $n=0$ mode is not included in this set because

*Paper 511, Bull. Am. Phys. Soc. 38, 1984 (1993).

[†]Invited speaker.

^{a)}Permanent address: Oak Ridge National Laboratory, Oak Ridge, Tennessee 37831.

it represents an instability that can in fact be controlled through the placement of external passive stabilizers supplemented by feedback control. Other low- n modes may also be stabilized by similar techniques. In order to simulate this effect we will designate β_{N3} , and β_{N3}^* as the threshold for instability with a conducting wall placed at a radius of 1.3 times the minor radius. This approximation of the effect of wall stabilization is supported by detailed analysis of the available superstructure in TPX for mode stabilization.⁵

In order to reduce the external current drive requirements, we seek to maximize the bootstrap current, I_{BS} . Ideally we would like to achieve $I_{BS}=I_p$, but any value approaching unity would greatly improve the chances of running the tokamak as a steady-state device. While increasing the bootstrap current it is imperative to examine its distribution and ensure that its profile is aligned with the profile which yields the best stability properties. The bootstrap fraction, $f_{BS}\equiv I_{BS}/I_p$ can be expressed as

$$f_{BS}=\epsilon^{1/2}\beta_{pol}C_{BS},$$

where ϵ is the inverse aspect ratio, $\beta_{pol}=4\pi^2a^2\langle p\rangle(1+\kappa^2)/\mu_0I_p^2$, and C_{BS} is a coefficient dependent on parameters which specify the current, density, and temperature profiles.

For fixed peakedness of the pressure profile f_{BS} increases as the self-inductance l_i increases. Here $l_i=2V\langle B_{pol}^2\rangle/(R\mu_0^2I_p^2)$. However, as l_i is increased, the bootstrap current profile peaks at increasingly larger radii, in terms of the normalized flux, leading to poor alignment with the desired current profile. A compromise must therefore be sought between these two opposing trends.

Some of the more important features of this dependency are increasing the peakedness of the density or temperature profile increases f_{BS} , however, the density profile has the stronger effect. Peaking the pressure profile causes I_{BS} to peak at a smaller radius. For fixed l_i , f_{BS} increases strongly with increasing density profile peakedness, the bootstrap alignment also improves. Details of these dependencies are available in Ref. 6.

II. RESULTS

A plasma equilibrium is specified by prescribing the plasma boundary shape and the pressure and parallel current density profiles, $p(\psi)$ and $(\langle J\cdot B\rangle/\langle B\cdot\nabla\phi\rangle)(\psi)$. Here ψ is the poloidal flux, normalized to have the value zero at the axis and unity at the plasma edge. The plasma shape is defined by

$$\begin{aligned}x &= R + a \cos(\theta + \delta \sin \theta), \\ z &= \kappa a \sin \theta.\end{aligned}\quad (1)$$

Here $R=2.25$ m, $a=0.5$ m, $\kappa=1.8$, and $\delta=0.5$.

The functional forms for the profiles are

$$\begin{aligned}p(\psi) &= p_0(1-\psi)^{\alpha_p}, \\ \frac{\langle J\cdot B\rangle}{\langle B\cdot\nabla\phi\rangle}(\psi) &= J_0(1-\psi^{\beta_J})^{\alpha_J} + \frac{\sigma d^2\psi(1-\psi)^2}{(\psi-a_0)^2+d^2}.\end{aligned}\quad (2)$$

The parameters p_0 , α_p , J_0 , α_J , β_J , σ , d , and a_0 , are used to vary the profiles. The functional forms for the pressure and the first term of the $\langle J\cdot B\rangle$ profile are familiar, the second term in the expression for $\langle J\cdot B\rangle$, enables shear reversal, by peaking the current off axis. In this term the coefficient a_0 helps determine the location of the peak in the current profile and thus indirectly the location of the minimum in the shear. Likewise σ , determines the degree of shear reversal, and d the width of the region of shear reversal.

In order to determine the bootstrap current we prescribe a temperature profile and compute the density profile from the pressure and temperature profiles. The temperature profiles for the electrons, T_e , and the ions, T_i , are such that $T_e=T_i=T(\psi)$, which has the form,

$$T(\psi) = T_0[\theta(1-\psi^{\beta_{T1}})^{\alpha_{T1}} + (1-\theta)(1-\psi^{\beta_{T2}})^{\alpha_{T2}}]$$

and the density profile is given as

$$n(\psi) = \frac{p(\psi)}{(1+\bar{Z}^{-1})T(\psi)}.$$

Here, $\bar{Z}\equiv n_e/n_i$ represents the average ion charge and is set equal to 1.25 and a $Z_{\text{eff}}=2.0$ was used for all the cases. Note that fixing the pressure and $\langle J\cdot B\rangle$ profiles determines the stability properties of an equilibrium. The temperature profile can therefore be varied to align the bootstrap current profile without affecting the stability properties.

Numerical accuracy plays an important role in the study of high- β advanced regime tokamaks. This is due partly to the strong magnetic shift and the resultant distortions of the flux surfaces, as well as due to the large gradients that are often encountered near the plasma edge. We have used the JSOLVER⁷ code to compute highly accurate equilibria.

The stability analysis was performed using several codes. These include the ideal MHD codes, PEST,⁸ CAMINO,⁹ and for analysis of resistive effects the PIES¹⁰ code.

In determining the β limit due to ballooning modes, we have used the criterion that *all* magnetic surfaces in the plasma satisfy this criterion.

We have examined a variety of equilibria and report the best results achieved for four main classes of equilibria. These will be referred to as the (a) conventional shear, (b) reversed shear, (c) ARIES-I,¹¹ and (d) ARIES-II¹¹ configuration. We will present detailed analysis for the first two cases and a brief summary of the latter two cases. We summarize the results for all four cases in Table I, details of each follow. The equilibrium profiles for the standard and reversed shear cases are shown in Figs. 1 and 2.

The optimization procedure involved: (a) selecting the exponent of the pressure profile, (b) adjusting the current profile to maximize the stable β , (c) adjusting the temperature profile to optimize the bootstrap current alignment, subject to the condition that the density profile is reasonable, i.e., avoiding hollow or very peaked profiles, with $(p_0/\langle p\rangle) > 2$. An exception to this requirement is the supersonic-type profiles which are not discussed here. This

TABLE I. Maximum stable β_N^* values for four configurations in TPX with the corresponding bootstrap fractions, f_{BS} . β_{N1}^* is the value with the conducting shell at $b = \infty$, and β_{N3}^* for $b = 1.3a$.

Configuration	β_{N1}^*	f_{BS}	β_{N3}^*	f_{BS}
Conventional shear	4.3	0.41	5.2	0.47
Reversed shear	2.5	0.39	6.8	0.92
ARIES-I	3.5	0.48	5.8	0.80
ARIES-II	3.3	0.50	7.0 ^a	1.0

^aRequires $b = 1.22a$.

procedure was then iterated to determine the optimal profiles. At each step as β is increased the entire procedure must be followed to ensure consistency. It should be noted that if we omit step (c) then the β limit increases above the values reported here. The requirement of bootstrap current alignment sets the limits in the choice of the pressure profile, both in shape and magnitude. In these studies generally we have attempted to keep the total current fixed for the particular class of equilibria under study, as we vary the other profile parameters to optimize the β limit.

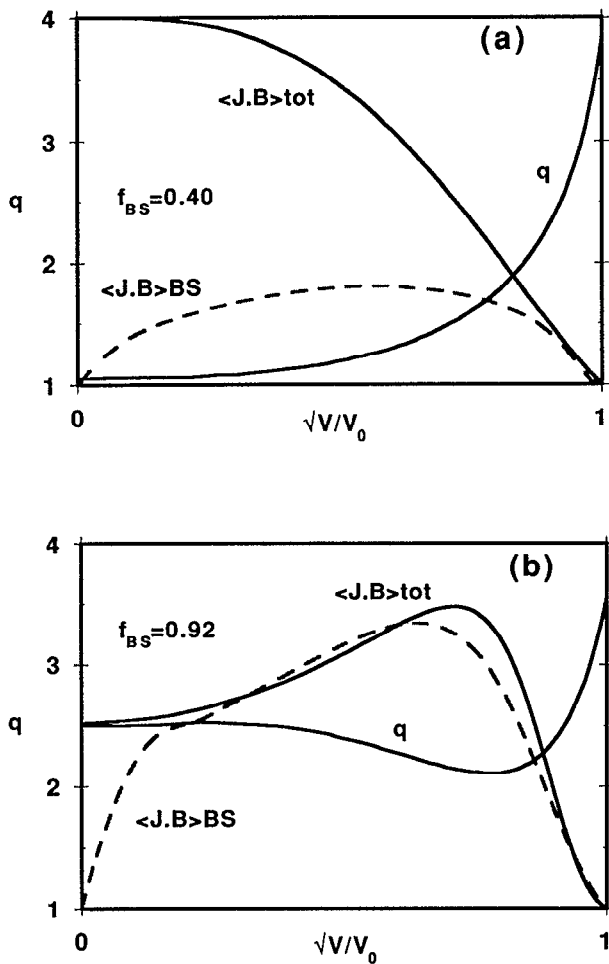


FIG. 1. Profiles of the total and bootstrap currents and the q profiles for (a) the conventional shear case and (b) the reversed shear case. The current profiles are plotted with the same arbitrary normalization selected to fit on the graph.

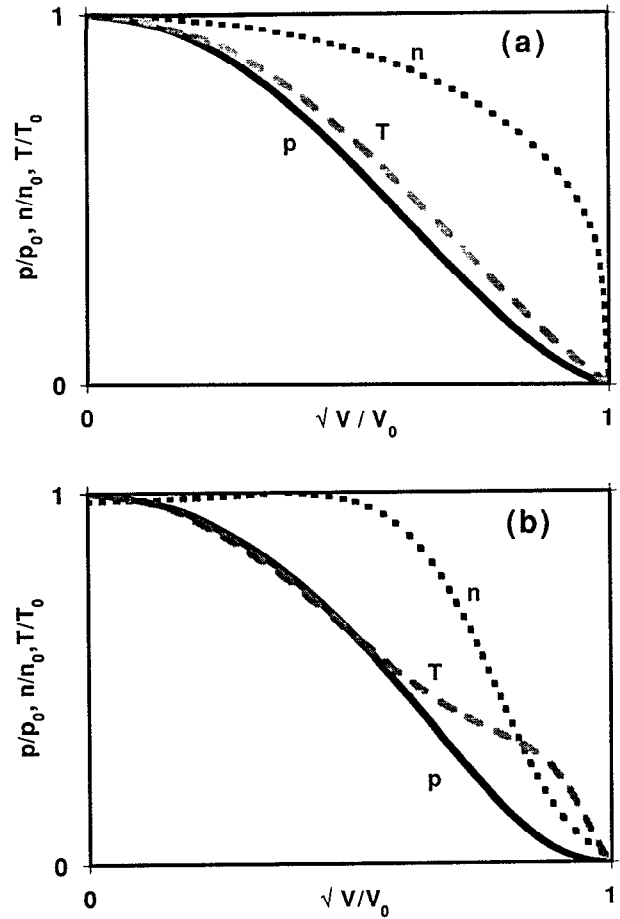


FIG. 2. Profiles of the pressure, temperature, and density profiles for (a) the conventional shear case and (b) the reversed shear case.

Conventional shear tokamak. This conforms to the conventional high- β , high-current, first stability mode of operation with $q_{axis} \sim 1$. The emphasis is on getting the highest β without violating the requirement of alignment of the bootstrap current. The profile parameters are $\alpha_p = 1.25$, $\alpha_J = 1$, $\beta_J = 1.525$, $\sigma = 0.0$, $\theta = 1.0$, $\alpha_{T1} = 1$, and $\beta_{T1} = 1.0$. Figure 3 shows the critical β , expressed in terms of β_N , for instabilities with $n = 1, 2, 3, 4$, and 5 . These are shown for boundary conditions corresponding to the wall at infinity, $b = \infty$, and at $b = 1.3a$. The region of stability lies below each curve. It is noted that only the points corresponding to integer n are meaningful. As expected, here the $n = 1$ external kink with $b = \infty$, has the lowest threshold with $\beta_N \approx 3.5$ which implies $\beta_{N1}^* \sim 4.3$. If the stabilizing influence of the wall is invoked, the β limit is determined by high- n ballooning modes, and is given by $\beta_N \approx 4.1$, corresponding to $\beta_{N3}^* \sim 5.2$. As mentioned earlier ignoring the bootstrap constraint allows higher stable β values, however, the resulting bootstrap current will exceed the optimal current locally, leading to a local overdrive. Experimentally this means that a compensating negative current will have to be driven in this region to restore the optimal current profile shape, clearly an undesirable situation.

Reversed shear tokamak. This mode seeks to maximize β^* and f_{BS} simultaneously with good alignment. It is

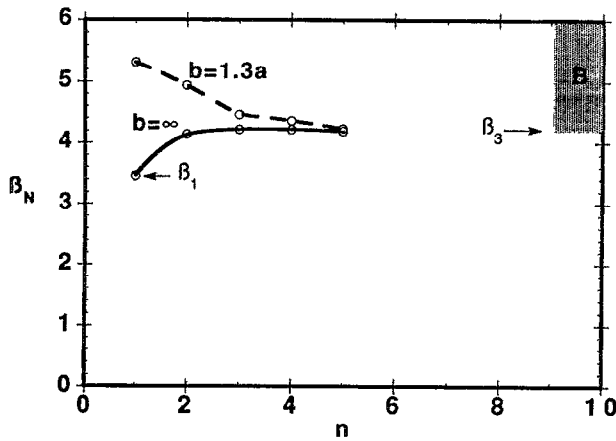


FIG. 3. Thresholds for onset of low- n external kinks with a conducting wall at infinity, solid curve, and at $b=1.3a$, broken curve, for the conventional shear case. The ballooning unstable region is shown by the shaded region marked B and is valid at $n = \infty$.

characterized by a hollow current profile leading to a non-monotonic q profile, see Fig. 1. The profile parameters are $\alpha_p=2.0$, $\alpha_j=1$, $\beta_j=1.0$, $\sigma=62.8$, $\theta=0.67$, $\alpha_{T1}=2.75$, $\beta_{T1}=1.0$, $\alpha_{T2}=1.5$, and $\beta_{T2}=8$. The shear reversal in the core of the discharge plays an important role in stabilizing high- n ballooning modes, and allows for a fairly peaked pressure profile, which is conducive to having a large bootstrap fraction with good alignment. The core region, the inner 75% in terms of the physical radius, has free access to the second stability regime while the outer, 25% region remains in the first stability regime. The $b = \infty$, low- n stability (see Fig. 4) is, however, quite restrictive and the $\beta_{N1}^* \approx 2.5$. Invoking wall stabilization dramatically raises the β limit above $\beta_N=5$, corresponding to $\beta_{N3}^* \approx 6.8$. In order to understand this relatively new mode of operation, we undertook several studies on the importance of different aspects of the reversed shear profiles. In particular we examined the role of q_{axis} , q_{min} , the location of q_{min} as well as

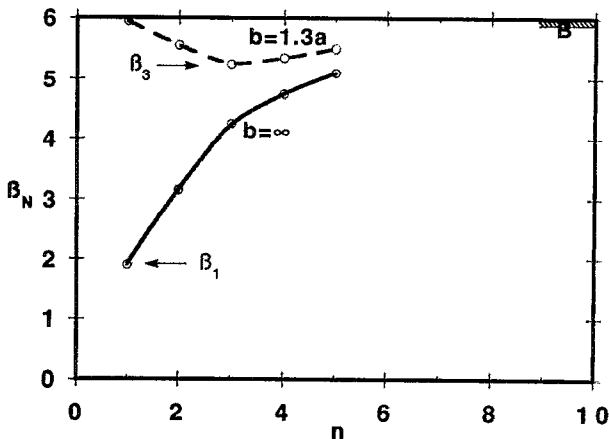


FIG. 4. Thresholds for onset of low- n external kinks with a conducting wall at infinity, solid curve, and at $b=1.3a$, broken curve, for the reversed shear case. The ballooning unstable region is shown as in Fig. 2.

the relative gradients in the shear. Some of the key findings were as follows. The choice of q_{min} plays a critical role, it is important to keep q_{min} greater than unity and preferably above 1.5 to avoid the $m/n=1/1$ mode, where m is the poloidal mode number. Keeping it above 1.5 helped to stabilize the 3/2 resistive mode. The role of q_{axis} was less critical, except for the requirement to keep $q_{axis} > q_{min}$ to ensure some degree of shear reversal. In the context of the $s-\alpha$ diagram,¹² this allows the core region of the plasma to pass in the negative s plane deep into the second-stable regime in terms of α , and then to return to low values of α when s becomes positive in the outer regions of the plasma. The location of the shear minimum plays a role in aligning the bootstrap fraction as well as in determining the stability to low- n external kinks, in the presence of the stabilizing shell. The external kink mode that is observed in these plasmas is a pressure-driven kink. This means that it has a strong coupling of the dominant external mode with non-resonant internal poloidal modes. This coupling is strongest in the vicinity of the minimum of the shear. Locating this minimum closer to the plasma edge makes these modes more susceptible to external shell stabilization.

ARIES-I. This mode of operation, similar to that used in the ARIES-I reactor study, gives a good compromise between high β and high β_p , which is required to raise the bootstrap fraction. The profiles are similar to those of the conventional shear scenario, except that q_{axis} is raised to 1.5 from unity. This improves stability to ballooning modes and also raises the bootstrap current. The profile parameters are $\alpha_p=2.0$, $\alpha_j=1$, $\beta_j=3.4$, $\sigma=0.0$, $\theta=1.0$, $\alpha_{T1}=1$, and $\beta_{T1}=1.0$. The β limits are $\beta_{N1}^*=3.5$ and $\beta_{N3}^*=5.8$; here $f_{BS}=0.8$ and the bootstrap alignment is reasonable.

ARIES-II. This configuration is designed to have direct access to second stability across the plasma cross section. The key here is to lower the plasma current to allow easy access to high β_p . It has $q_{axis} \geq 2$, peaked current and pressure profiles and has $I_{BS}/I_p \sim 1$. Note that the second stable regime lies above an unstable region for $3.5 \leq \beta_N \leq 4.8$. The profile parameters are, $\alpha_p=1.5$, $\alpha_j=1$, $\beta_j=1.325$, $\sigma=0.0$, $\theta=1.0$, $\alpha_{T1}=1.5$, and $\beta_{T1}=1.0$. The β limits are $\beta_{N1}^*=3.3$ and $\beta_{N3}^*=7.0$, and $f_{BS}=1$. This configuration has the lowest plasma current (≈ 1 MA). Consequently even though β_N^* may be large, the absolute value of β^* is low, equal to 3.2. Note also that the external shell requirements are more stringent with the effective wall distance being 1.22.

To assess tearing mode stability we have used the three-dimensional PIES code to calculate the saturated island widths for a conventional shear profile and a reversed shear profile. This study shows that the reversed shear configuration is surprisingly robust and develops fewer and smaller islands compared to the conventional shear case, see Fig. 5. The conventional shear case shows a strong 2/1 mode which in turn drives islands near the $q=3$ and $q=4$ surfaces, so that the outer portion of the tokamak becomes stochastic as about 30% of the plasma cross-section fills with islands. This was observed at a relatively low value of $\beta=1\%$. Increasing the pressure causes more deterioration of the surfaces which puts the problem beyond the scope of

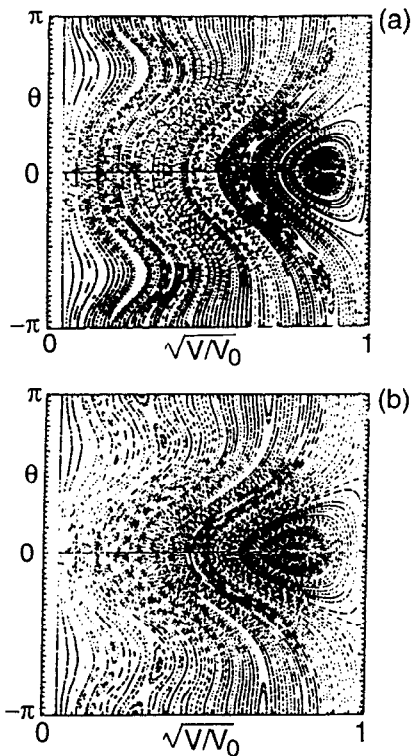


FIG. 5. Poincaré plots of the magnetic field showing the three-dimensional saturated equilibrium state for (a) the conventional shear, at $\beta=1\%$, and (b) the reversed shear configurations, at $\beta=3\%$. Note that at much higher β the reversed shear configuration has fewer and smaller islands.

our calculation. In contrast, at β of 3%, in the reversed shear case, we observe a modest 5/4 island and no evidence of the numerous higher- n islands observed in the conventional profile case. This study gives a clear indication that the reversed shear profile also has superior tearing mode stability as compared to the conventional shear profile.

III. DISCUSSION

In this study we have identified several configurations with the potential of operating as advanced regime tokamaks. We have examined their MHD stability and shown that stable profiles with bootstrap fractions close to unity with good alignment are achievable at high β_N^* values. They hold the promise of economical steady-state reactors. A major unresolved issue is the role of external boundary conditions to stabilize the kink modes in steady-state operation. Experiments in DIII-D¹³ and Princeton Beta Experiment (PBX-M), have indicated¹⁴ that this may be a justified assumption. However, more work is required in this area. Theoretical results in this area will be presented at a later date.

The reversed shear mode is of particular interest as it has other favorable features. A study¹⁵ of toroidal drift modes shows that the reversed shear configuration has superior microinstability properties, with promising implications for transport behavior. These results combined with

the MHD stability described above make this a promising candidate for a steady-state configuration. Finally, we note that several experiments^{16,17} have demonstrated various aspects of the reversed shear configuration, indicating that accessing this regime is a practical possibility.

ACKNOWLEDGMENTS

The authors would like to thank the TPX group for their support. This work is funded by U.S. Department of Energy under Contract No. DE-AC02-76-CHO-3073.

- ¹M. W. Phillips, M. H. Hughes, A. M. M. Todd, J. T. Hogan, R. A. Dory, F. J. Helton, J. M. Greene, J. W. Helton, S. C. Jardin, J. L. Johnson, J. Manickam, R. R. Parker, and N. Pomphrey, *12th International Conference on Plasma Physics and Controlled Nuclear Fusion Research*, Nice, France, 1988 (International Atomic Energy Agency, Vienna, 1989), Vol. 2, p. 65.
- ²W. Howl, A. D. Turnbull, T. S. Taylor, L. L. Lao, F. J. Helton, J. R. Ferron and E. J. Strait, *Phys. Fluids B* **4**, 1724 (1991).
- ³H. Naitou and K. Yamazaki, *Nucl. Fusion* **28**, 1751 (1988).
- ⁴R. J. Goldston and the TPX team, *Proceedings of the 20th European Physical Society Conference on Controlled Fusion and Plasma Physics*, Lisbon, 1993, edited by J. A. Costa Cabral, M. E. Manso, F. M. Serra, and F. C. Schuller (European Physical Society, Petit-Lancy, 1993), p. I-80.
- ⁵M. S. Chance, J. Bialek, S. C. Jardin, C. Kessel, J. Manickam, and H. Neilson, *Bull. Am. Phys. Soc.* **38**, 2050 (1993).
- ⁶N. Pomphrey, "Bootstrap dependence on plasma profile parameters," submitted to *Nucl. Fusion*.
- ⁷J. Delucia, S. C. Jardin, and A. M. M. Todd, *J. Comput. Phys.* **37**, 183 (1980).
- ⁸R. C. Grimm, R. L. Dewar, and J. Manickam, *J. Comput. Phys.* **49**, 94 (1983).
- ⁹M. S. Chance, *Proceedings of the Workshop on Theory of Fusion Plasmas*, Varenna, 1987, edited by A. Bondeson, E. Sindoni, and F. Troyon (Editrice Compositori, Bologna, 1988), p. 87.
- ¹⁰A. H. Reiman and H. S. Greenside, *Comput. Phys. Commun.* **43**, 157 (1986).
- ¹¹F. Najmabadi, R. W. Conn, and the ARIES team, *Proceedings of the 13th Symposium on Fusion Engineering*, Knoxville, Tennessee, 1989 (Institute of Electrical and Electronic Engineers, Piscataway, NJ, 1990), p. 1021.
- ¹²J. W. Connor, R. J. Hastie, and J. B. Taylor, *Phys. Rev. Lett.* **40**, 396 (1978).
- ¹³E. J. Strait, L. L. Lao, T. S. Taylor, M. S. Chu, J. K. Lee, A. D. Turnbull, S. L. Allen, N. H. Brooks, K. H. Burrell, R. W. Callis, T. N. Carlstrom, M. S. Chance, A. P. Colleraine, D. Content, D. C. DeBoo, J. R. Ferron, J. M. Greene, R. J. Groebner, W. W. Heidbrink, F. J. Helton, D. N. Hill, R.-M. Hong, N. Hosogane, W. Howl, C. L. Hsieh, G. L. Jackson, G. L. Jahns, A. J. Kellman, J. Kim, S. Kinoshita, E. A. Lazarus, P. J. Lomas, J. L. Luxon, M. A. Mahdavi, Y. Neyatani, T. Ohkawa, T. H. Osborne, D. O. Overskei, T. Ozeki, M. Perry, P. I. Petersen, T. W. Petrie, J. C. Phillips, G. D. Porter, D. P. Schissel, J. T. Scoville, R. P. Seraydarian, M. Shimada, T. C. Simonen, R. T. Snider, R. D. Stambaugh, R. D. Stav, H. St. John, R. E. Stockdale, U. Stroth, and R. Wood, in Ref. 1, Vol. 1, p. 83.
- ¹⁴N. Sauthoff, N. Asakura, R. Bell, M. Chance, P. Duperrex, J. Faunce, H. Fishman, R. Fonck, G. Gammel, G. Greene, R. Hatcher, P. Heitzenroeder, A. Holland, S. Jardin, T. Jiang, R. Kaita, S. Kaye, C. Kessel, T. Kozub, H. Kugel, D. Kungl, B. LeBlanc, F. Levinton, J. Manickam, M. Okabayashi, M. Ono, S. Paul, E. Powell, Y. Qin, D. Roberts, S. Schweitzer, S. Sesnic, S. Bernabei, and H. Takahashi, *13th International Conference on Plasma Physics and Controlled Nuclear Fusion Research*, 1990 Washington, DC (International Atomic Energy Agency, Vienna, 1991), Vol. 1, p. 709.
- ¹⁵C. Kessel, J. Manickam, G. Rewoldt, and W. Tang, *Phys. Rev. Lett.* **72**, 1212 (1994).
- ¹⁶JET team, *14th International Conference on Plasma Physics and Controlled Nuclear Fusion Research*, Würzburg, Germany, 1992 (International Atomic Energy Agency, Vienna, 1993), Vol. 1, p. 15.
- ¹⁷DIII-D team, in Ref. 16, Vol. 1, p. 41.